Angewandte Chemie
Eine Zeitschrift der Gesellschaft Deutscher Chemiker

Supporting Information

Signaling in Systems Chemistry: Programing Gold Nanoparticles Formation and Assembly Using a Dynamic Bistable Network

Indrajit Maity, Dharm Dev, Kingshuk Basu, Nathaniel Wagner, and Gonen Ashkenasy**

anie_202012837_sm_miscellaneous_information.pdf

Supporting Information

Table of Contents

1. Materials and general characterization methods

Chemicals and reagents were purchased from Sigma Aldrich or Merck. Amino acids, resins and coupling reagents were purchased from Alfa Assar and Novabiochem. DMF (peptide synthesis grade) was purchased from biotech. $AuCl_3$ salt was provided by Prof. Nurit Ashkenasy, Department of Materials Engineering, Ben-Gurion University of the Negev. All the peptides (Electrophile: **E, E_S;** Nucleophile: **N, N_β , N_S;** Replicator: **R, R_β , R_S)** were synthesized on solid phase as described before.[1-3] All compounds were purified using a preparative HPLC (Dionex Ultimate 3000 instrument) with a C18 reverse phase preparative column at a flow rate of 20 mL/min. The purity of the compounds was checked by Analytical HPLC (Dionex 1100) with a reverse phase C18 column at a flow rate of 1.5 mL/min. Mass spectrometry analysis was performed by LCMS Thermo Surveyor 355. The kinetics of the bistable reaction, indicating when steady state was reached, was analyzed by using UPLC (Waters Acquity) with a C18 column at a flow rate of 0.3 mL/min.

The aggregation kinetics of Au nanoparticles was recorded using a Cary 60 UV-Vis spectrophotometer. The size and shape of the Au nanoparticles were investigated by high-resolution transmission electron microscope (FEI Tecnai 12 TWIN TEM) operated at an accelerating voltage of 120 kV. In order to prepare samples for imaging studies, the steady state mixtures containing Au NPs were diluted and well mixed into double distilled water with vortex (30s for the morphology study; 40s to control the shape; 5s for self-assembly), yielding a final Au NPs concentration of 5 μM. First, 10 μL of each sample was drop casted on a TEM copper grid with a 300-mesh carbon support (Electron Microscopy Sciences). Then, after a few minutes (15 min for the morphology study; 5 min to control the shape or self-assembly), excess solution was wicked away with a filter paper and the grids were placed in a desiccator to dry under vacuum for 24 hours.[4]

2. Characterization of the bistable reaction network steady states

Stock solutions of the electrophiles (**E** and **E_S)**, Nucleophiles (**N, N_β** and **N_S**) or Replicators (**R, R_β** and **R_S)** were prepared by dissolving the lyophilized compounds in double distilled water in 1.5 mL Eppendorf, yielding stock concentrations of 0.5 - 2 mM. The replication reactions were carried out by mixing together **E**, **N**, **R**, the small molecule thiol **S** (2-Mercapto-ethanesulfonate sodium salt), 4-acetamidobenzoic acid (ABA) as internal standard and tris (2-carboxyethyl) phosphine hydrochloride (TCEP).[2] These reactions were initiated with variable concentration combinations of **E**, **N** and **R,** while always providing equal concentrations of **E** and **N** and keeping the total peptides concentration ([**E**+**R**] or [**N**+**R**]) constant at 100 ±10 μM. The small molecule thiol **S** was added in excess amount (0.5 mM) in all cases. The final concentration of ABA and TCEP in the reaction mixture were 50 μM and 4 mM, respectively.

The network reaction experiments were initiated by the addition of MOPS buffer [3-(N-morpholino) propanesulfonic acid; 500 mM, pH 7] to the above mixtures; the reaction temperature was maintained at 22 °C in Julabo chiller. TCEP (0.15-0.20 μL of 1.1 M solutions) was continuously re-supplied to the system in 24 hours intervals. Aliquots (5 μL) were taken at designated time points, immediately quenched in 20% glacial acetic acid mixture in water and stored frozen until subjected to RP-UPLC analysis. The reactions were allowed to continue until they reached long lived steady states. Then, the steady state (SS) concentration for each compound (**E**, **N** and **R**) was calculated by averaging the final concentrations at three different time points (t ≥ 72h). The apparent steady state values (K_{app}) were calculated by using K_{app} = ([**R**][**S**]/[**E**][**N**]).[3] The experiments with **R_β** and **R_S** based networks were performed, analyzed

and processed in the same manner. All experiments were performed at least in duplicates to minimize the experimental error.

The Hss-to-Lss switching experiment started by incubating 100 μM of **R** at 37 °C for 2 days, while keeping all other parameters unchanged. The system was then allowed to react at 22 °C for 4 more days. The final K_{app} values were estimated by the above described method, and indeed was found to be in the 'low' SS regime. The Lss-to-Hss switch was initiated with 10 μM of **R** and 90 μM (each) of **E** and **N**, incubated for 3 days at 37 °C without the small molecule thiol **S**. Thereafter, the small molecule thiol **S** was added into the reaction mixture, which was allowed to react at 22 °C for 3 more days. The final K_{app} values were calculated and found in the 'high' SS regime. Note the initial stage of this latter assay, equilibration in higher temperature in absence of **S**, resulted in somewhat faster hydrolysis of the **E** and **R** thioesters (≤ 15% over 3 days).

3. Regulating nanomaterial structural features by the network SS solutions

3.1 *In-situ nanoparticle synthesis to control morphology*

As described above (Section 2), the bistable reaction network (either based on **R** or $\mathbf{R_\beta}$) yields either the high steady state (Hss) or low steady state (Lss) mixtures. $AuCl_3$ salt and a freshly prepared $NaBH_4$ solution were mixed with the respective SSs (obtained after 72 h), where the final concentrations of Au^{+3} salt and $NaBH_4$ were maintained as 15 μM and 500 μM, respectively. The reaction mixture was first vortexed for 30 s and then kept undisturbed. Subsequently, Au nanoparticle (Au NP) samples were prepared at various time points during the above experiment for TEM analysis to visualize the NP morphology. The same experiment (with the **R** based network) was repeated with Au^{+3} salt concentration of 5 μM. The diameter of the observed nano-urchins, and length of hyperbranched nanorod aggregates, were estimated manually by analyzing the respective TEM images. Similar, in-situ nanoparticles synthesis experiment was also performed with the single equilibrium state, obtained from the **Rs** based network, and investigated by transmission electron microscope.

3.2 *Formation of non-metallic nanoparticles*

The Au salt concentrations (5 μM and 15 μM) in the above performed experiments were initially assumed too small to show the surface plasmon resonance (SPR) peak due to low concentration of synthesized Au NPs. However, the increase of the Au salt concentration (30 μM) in the similar experiments with respective Hss and Lss, also remained UV-Vis silent **(Fig. s4A).** Consequently, a series of control experiments were performed as following to understand this issue. In **Fig. s4B,** a clear SPR peak at 530 nm was observed when the NPs were synthesized by reducing $AuCl_3$ with $NaBH_4$ (500 μM) in water while a weak signal at 575 nm was seen when the NPs were synthesized in MOPS buffer without any reducing agent. But those NPs remained undetectable by UV-Vis spectroscopy which were synthesized by fast reduction of $AuCl_3$ with $NaBH_4$ in MOPS buffer containing 500 μM of MESNA corresponding to similar concentration in the bistable reaction network. Similar experiments with increased Au salt concentrations (up to 200 μM) proportionally increased the concentrations of synthesized Au NPs. But still the UV-Vis spectroscopy remained unable to detect the NPs **(Fig. s4C)** which clearly demonstrates the emergence of non-metallic, ultra-small Au NPs by fast reduction process with $NaBH_4$ in presence of excess MESNA (500 μM). Therefore, the in situ synthesized NPs in respective SSs solutions are non-metallic and they do not possess any SPR band.

3.3 *Regulating NP shapes and self-assembly kinetics*

Au NP seeds were synthesized by mixing in 1:1 ratio (v/v) of the Good-buffer MOPS (3-(N-morpholino) propanesulfonic acid; 500 mM, pH 7) and Au salt solution (4.5 mM). This mixture leads to generate the transient red colored spherical seeds upon 30s of vortex, while after continuous vortex for additional 30s the red seeds were spontaneously transformed into the blue colored seeds which contains mixture of anisotropic Au NPs. The syntheses of both types of seeds were characterized by UV-Vis spectroscopy and the shapes of the seeds were analyzed from the respective TEM images (**Fig. s11**).

Then, in order to control the shape and self-assembly of NP seeds by the bistable reaction networks, the respective high and low steady state mixtures were collected at 72 h from the bistable reaction. Thereafter, the fresh pre-synthesized nanoparticles seeds (either red seeds or blue seeds) were immediately cultured into the Hss or Lss separately and kept them undisturbed during the nanoparticle growth and self-assembly process. The concentrations of both seed types were maintained in these experiments at either 100 μM or 30 μM. Subsequently, Au NP samples were prepared for TEM analysis to investigate the shapes of nanoparticles. The samples containing Au NPs were diluted and then well mixed into double distilled water by sonication (10s) and vigorous vortexing (40s). The distribution of several shaped nanoparticles was then estimated by manual counting from the respective TEM images. Further, UV-Vis spectroscopy was used to follow the self-assembly kinetics. Therefore, first the above stated experiment was set in 1.5 mL Eppendorf, and then 100 μL of respective reaction mixture was immediately transferred into the UV cuvette to follow the aggregation of nanoparticles in respective SS mixture by using UV-Vis spectroscopy. Moreover, we have performed the Hss-to-Lss and Lss-to-Hss switch experiments (see section 2), and then employed the switched mixtures to control the assembly of the Au NPs. TEM microscope and UV-Vis spectroscopy were used (using the above described procedure) to investigate the resulted self-assembly structures. Using HPLC experiments, we revealed that the network components (**E**, **N** and **R**) were all stable against degradation (or other reactions) during exposure to the Au NPs, and consequently that the compound distribution in the ss mixtures remained practically unchanged during the entire experiment **(Fig. s16).**

In order to get more insight into which network components are more effective for the Au NPs surface functionalization, we performed a ligand exchange experiment. The Au blue seeds were cultured into the Lss mixture and allowed to equilibrate for 24 h. Next, the resulted heterogenous mixture was centrifuged (15 min at 8000 rpm) and the supernatant solution was discarded. The blue seeds at bottom of the centrifuged Eppendorf were thoroughly washed (4 times) with distilled water and centrifuged again. These blue seeds, functionalized with network components, were then dispersed in mixture containing an excess of thiol molecule (3-mecaptopropanoic acid; 4 mM) to allow ligand exchange reaction for 12 h at 25 °C. Following the ligand exchange, the solution was again centrifuged for 30 min at 8000 rpm and the supernatant was collected and subjected to LCMS (liquid chromatography mass spectrometry) measurements for characterization.

4.Table s1: Bistable network reaction experiments and the corresponding K_{app} values

Case-Entry	$^{1}[R]_{t=0}$ (μM)	$^{1}[E]_{t=0}$ (μM)	$^{1}[N]_{t=0}$ (μM)	$^{2}[R]_{ss}$ (μM)	$^{2}[E]_{ss}$ (μM)	$^{2}[N]_{ss}$ (μM)	$[S]_{ss}$ (μM)	K_{app}	Remarks
1.	94.5	0	0	84.4	5.3	7.3	584	**1280**	**R**-based network
2.	96.7	0	0	80	5.4	8	580	**1070**	
3.	96	6.3	4.9	85.6	6	5.3	586	**1580**	
4.	96	6.3	4.5	85.9	6.4	5.8	586	**1360**	
5.	90	9	5	86.4	8	5	586	**1270**	
6.	8.5	88	92	70.8	9	24	571	**187**	
7.	13	76.5	86.5	69.6	8.8	23.8	570	**189**	
8.	45	43	52	70.4	8.5	19.1	570	**247**	
9.	46	43.5	49	70.8	7.4	18.3	571	**298**	
10.	43.5	46.4	46.8	72.3	8.2	17.1	572	**295**	
11.	90	0	0	53.8	22.8	21.6	553.8	**60.6**	**R_{β}**-based network
12	90.8	5.4	6.2	62.3	21.0	20.6	562.3	**81**	
13	9	94.8	86.5	25.6	64.5	65.2	525.6	**3.2**	
14	10.2	84.9	87.4	29.8	61.6	63.7	529.8	**4**	
15	90.2	0	0	9.8	64.3	74.5	509.8	**1**	**Rs**-based network
16	95	0	0	8.4	60.7	73	508.4	**0.96**	
17	8.4	100	93.3	8.8	68.4	77.2	508.8	**0.84**	
18	9.8	103	83	7.6	74.3	70.2	507.6	**0.74**	
19	90.1	0	0	66	8.9	10.7	566	**392**	Hss-to-Lss Switch
20	92.3	0	0	72.3	9.8	10.3	572.3	**410**	
21	8.4	87.3	76.2	72.7	6.5	6	572.2	1055	Lss-to-Hss switch
22	7.6	94.9	84.9	73.1	6.2	5.7	573.1	**1185**	

Reaction conditions: The total [peptide] = 100 μM, temperature = 22 °C , thiol concentration = 500 μM. [1] $[R]_{t=0}$, $[E]_{t=0}$ and $[N]_{t=0}$ indicate initial concentration of replicator, electrophile and nucleophile at t = 0 minutes of the replication reaction. [2] $[R]_{ss}$, $[E]_{ss}$, $[N]_{ss}$ and $[S]_{ss}$ represent the average concentration of replicator, electrophile, nucleophile and small thiol molecule at the steady state. We note that in the Lss mixtures, the electrophile concentration is lower than the nucleophile concentration, due to 2-8% electrophile hydrolysis during the experiments. The *Red* values refer to Hss and *Blue* values to Lss.

5. Additional figures

5.1 Controlling the morphology of Au nanoparticles

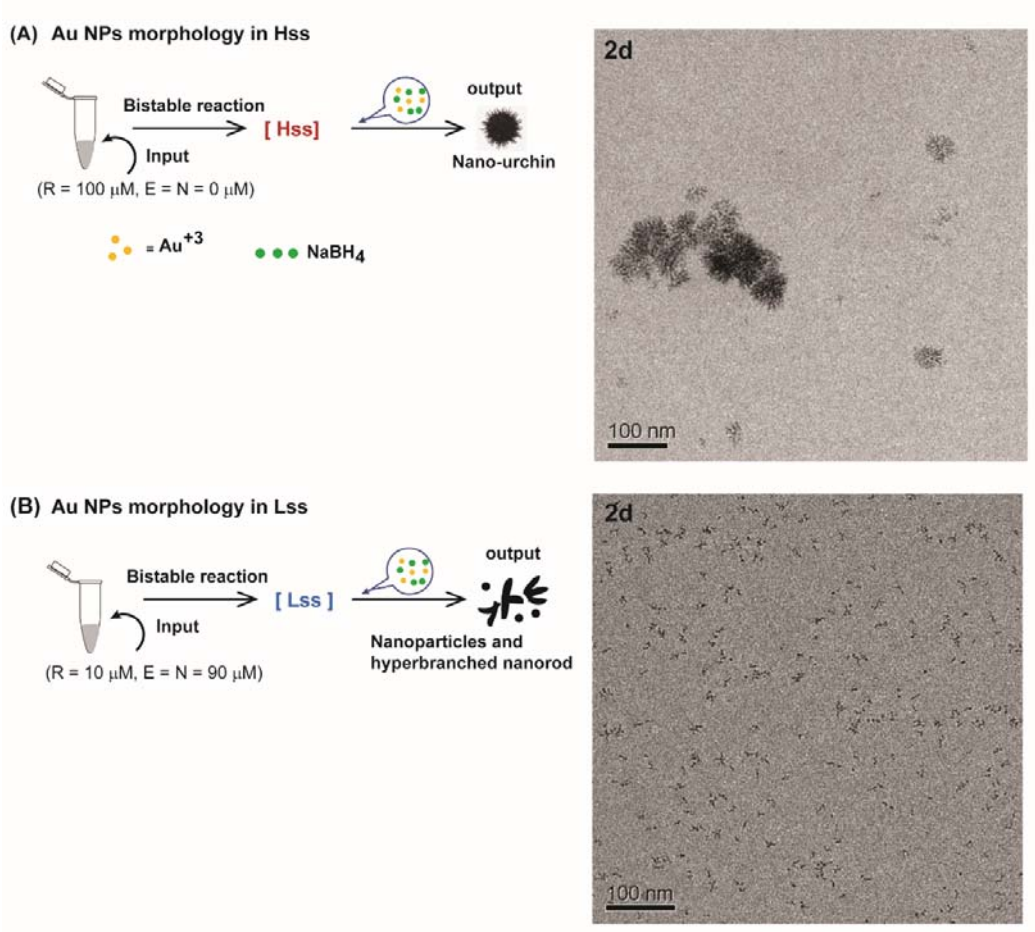

Figure s1. (A) Replication reaction initiated with 100 μM **R** yielding the Hss mixture, which is then used to synthesize Au NPs presenting the nano-urchin morphology. Transmission electron microscope image displays the well-defined nano-urchin aggregates obtained after 2 days in the Hss. **(B)** Replication reaction initiated with 10 μM of **R** and 90 μM (each) of **E** and **N** yielding the Lss mixture, which is used to synthesize Au NPs presenting the hyperbranched nanorod morphology. The TEM image displays ultra-small nanoparticles and hyperbranched nanorod structures after 2 days in the Lss. In all experiments, the Au salt and $NaBH_4$ concentrations were maintained as 15 μM and 500 μM, respectively. Experiments were carried out at room temperature (RT; 22 °C).

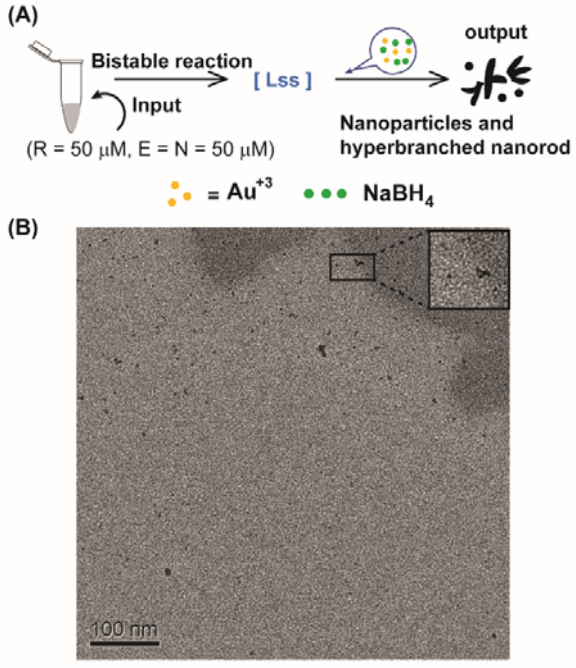

Figure s2. (A) Replication reaction initiated with 50 μM of **R** and 50 μM (each) of **E** and **N,** yielding the Lss mixture, which is used to synthesize Au NPs presenting the hyperbranched nanorod morphology. **B)** TEM image displays ultra-small nanoparticles and hyperbranched nanorod structures after 2 days in the Lss. Au salt and $NaBH_4$ concentrations were maintained as 15 μM and 500 μM respectively. Experiments were carried out at room temperature (RT; 22 °C).

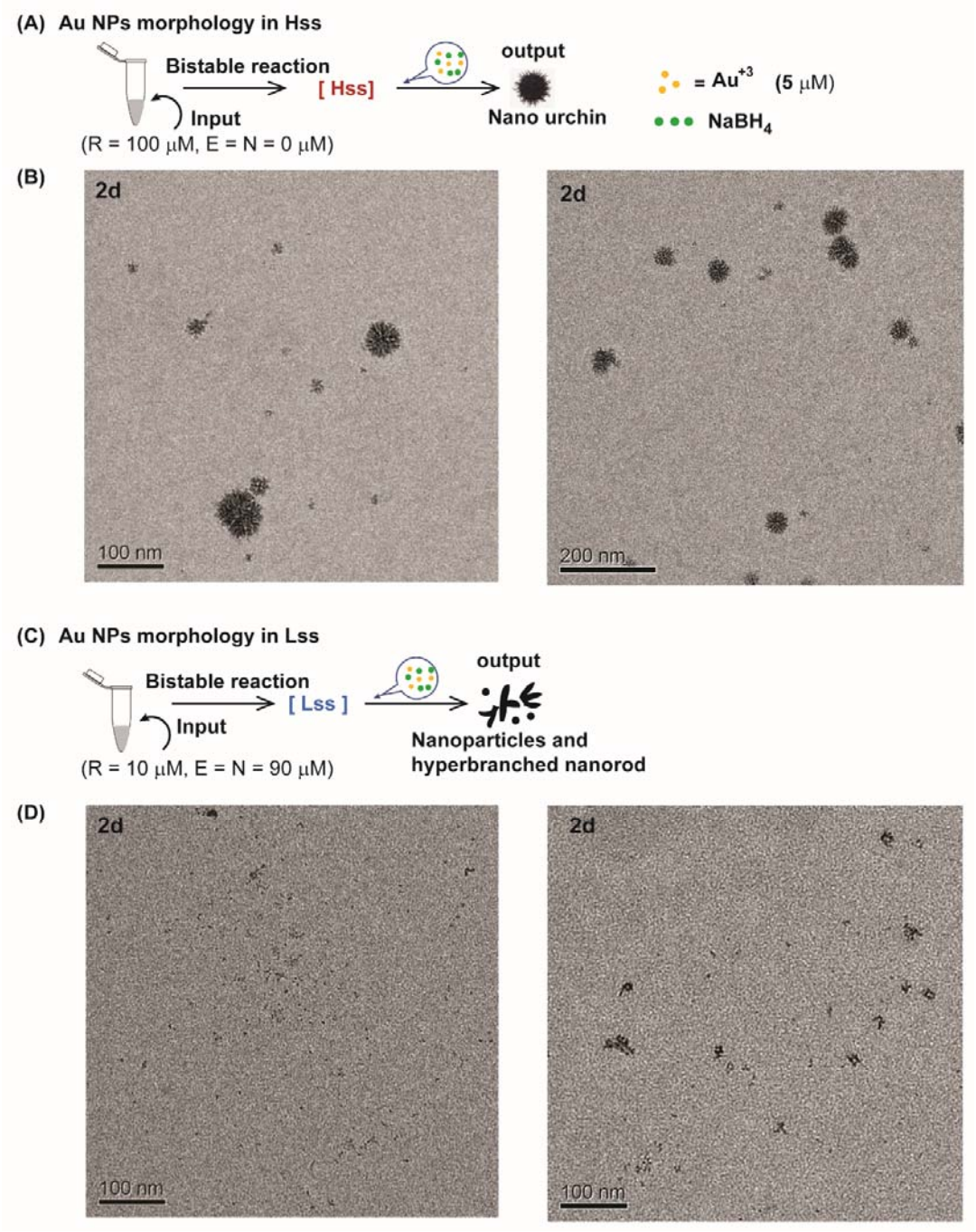

Figure s3. (A) Replication reaction initiated with 100 μM **R** yielding the Hss, which is used to synthesize Au NP of nano-urchin morphology. **(B)** TEM images showing the well-defined nano-urchin aggregates after 2 days in the Hss. **(C)** Replication reaction initiated with 10 μM of **R** and 90 μM (each) of **E** and **N** gives the Lss, which is used to synthesize Au NP of hyperbranched nanorod morphology. **(D)** TEM images showing ultra-small nanoparticles and well-defined hyperbranched nanorods after 2 days in the Lss. In all experiments, the Au salt and $NaBH_4$ concentrations were maintained as 5 μM and 500 μM respectively. Experiments were carried out at room temperature (RT; 22 °C).

5.2 Formation of non-metallic nanoparticles

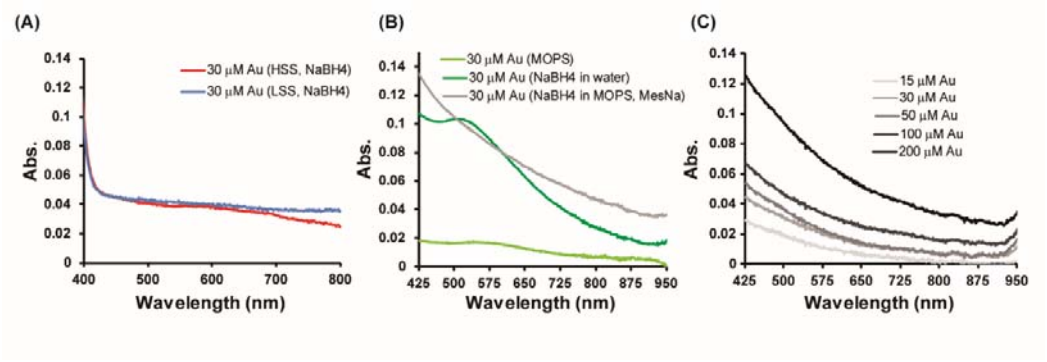

Figure s4. (A) UV-Vis spectra obtained for non-metallic Au NPs, generated by reduction with $NaBH_4$ inside the bistable reaction Lss and Hss mixtures. The final concentration of Au salt in these experiments was maintained at 30 μM. **(B)** UV-Vis spectra of Au NPs obtained in control experiments, where the NP synthesis was carried out with the reducing agent $NaBH_4$, either in water or mixture of MOPS buffer and MESNA (0.5 mM), or in MOPS buffer only without the reducing agent. **(C)** UV-Vis spectra of the non-metallic Au NPs. The data shows that the NP remained UV-Vis silent also when the Au salt concentration was raised from 15 μM up to 200 μM. For this case, Au NPs were synthesized by reducing $AuCl_3$ with $NaBH_4$ (500 μM) in MOPS buffer containing 500 μM of MESNA.

5.3 Controlling the morphology of Au nanoparticles using the bistable R_β networks

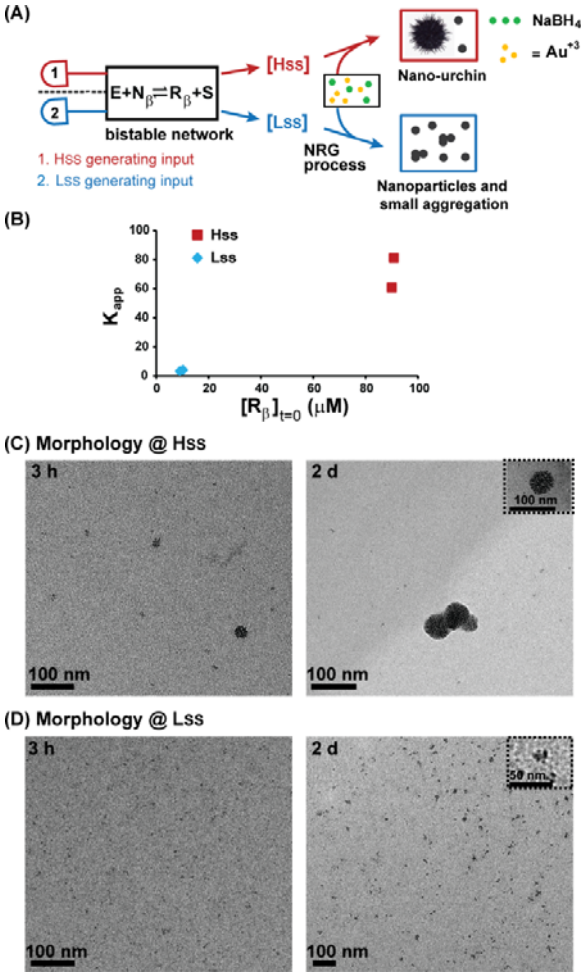

Figure s5. (A) General experimental layout of the **Rs** based cascade reaction configuration. **(B)** Representative results highlighting bistability in the SS product distribution (manifested by Kapp; **Table s1**). ***(C)*** TEM images obtained after applying the SS of a replication reaction initiated with 100 μM $\mathbf{R_\beta}$ - yielding the Hss mixture – in order to synthesize Au NPs. Images display the well-defined nano-urchin aggregates obtained after 2 days in the Hss. **(D)** TEM images obtained after applying the SS of a replication reaction initiated with 10 μM of $\mathbf{R_\beta}$ and 90 μM (each) of **E** and $\mathbf{N_\beta}$ - yielding the Lss mixture – in order to synthesize Au NPs. Images display the ultra-small nanoparticles obtained after 3h and small aggregated structures obtained after 2 days in the Lss. In all experiments, the Au salt and $NaBH_4$ concentrations were maintained at 15 μM and 500 μM, respectively. Experiments were carried out at room temperature (RT; 22 °C) in buffered pH =7.

5.4 Controlling the morphology of Au nanoparticles by (single state) Rs based networks

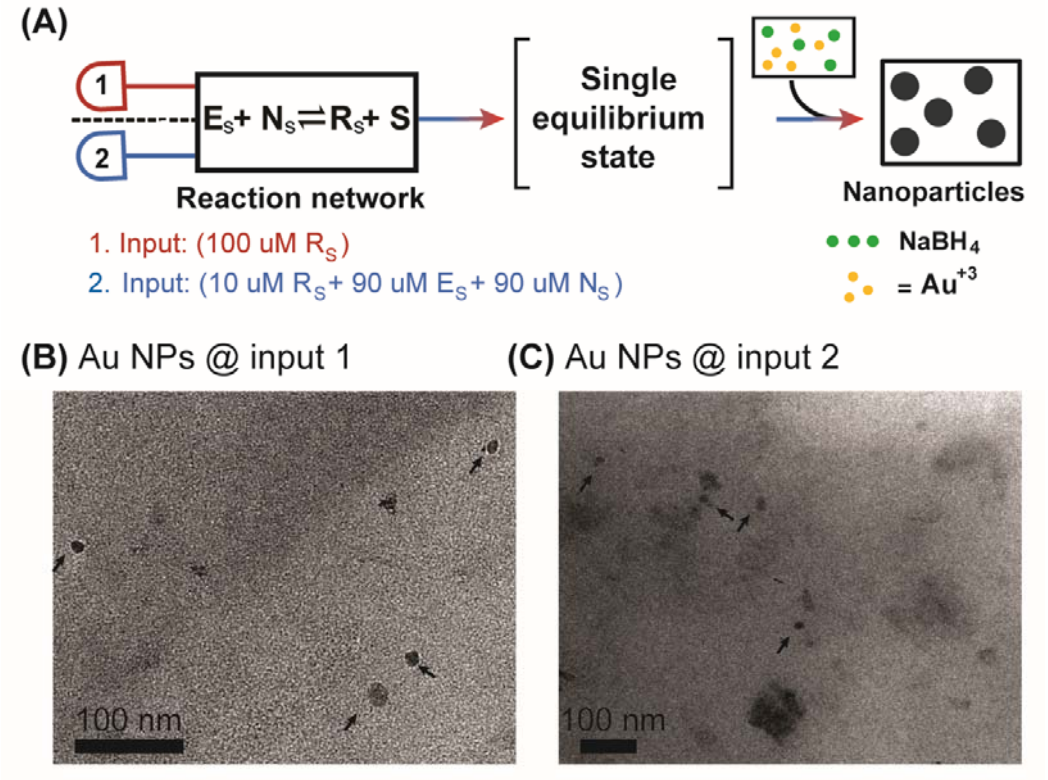

Figure s6. (A) General experimental layout of the **Rs** based cascade reaction configuration. Experiments with four different initial concentration combinations resulted in very similar SS product distributions (**Table s1**). **(B)** TEM images obtained after applying the SS of a ligation reaction initiated with 100 μM **R_S** to synthesize Au NPs for 2 days. **(C)** TEM images obtained after applying the SS of a ligation reaction initiated withn10 μM of **R_S** and 90 μM (each) of **E_S** and **N_S** to synthesize Au NPs for 2 days. In all experiments, the Au salt and $NaBH_4$ concentrations were maintained at 15 μM and 500 μM, respectively. Experiments were carried out at room temperature (RT; 22 °C) in buffered pH =7.

5.5 Control experiments for studying the morphology of Au NPs synthesized in presence of N or S only

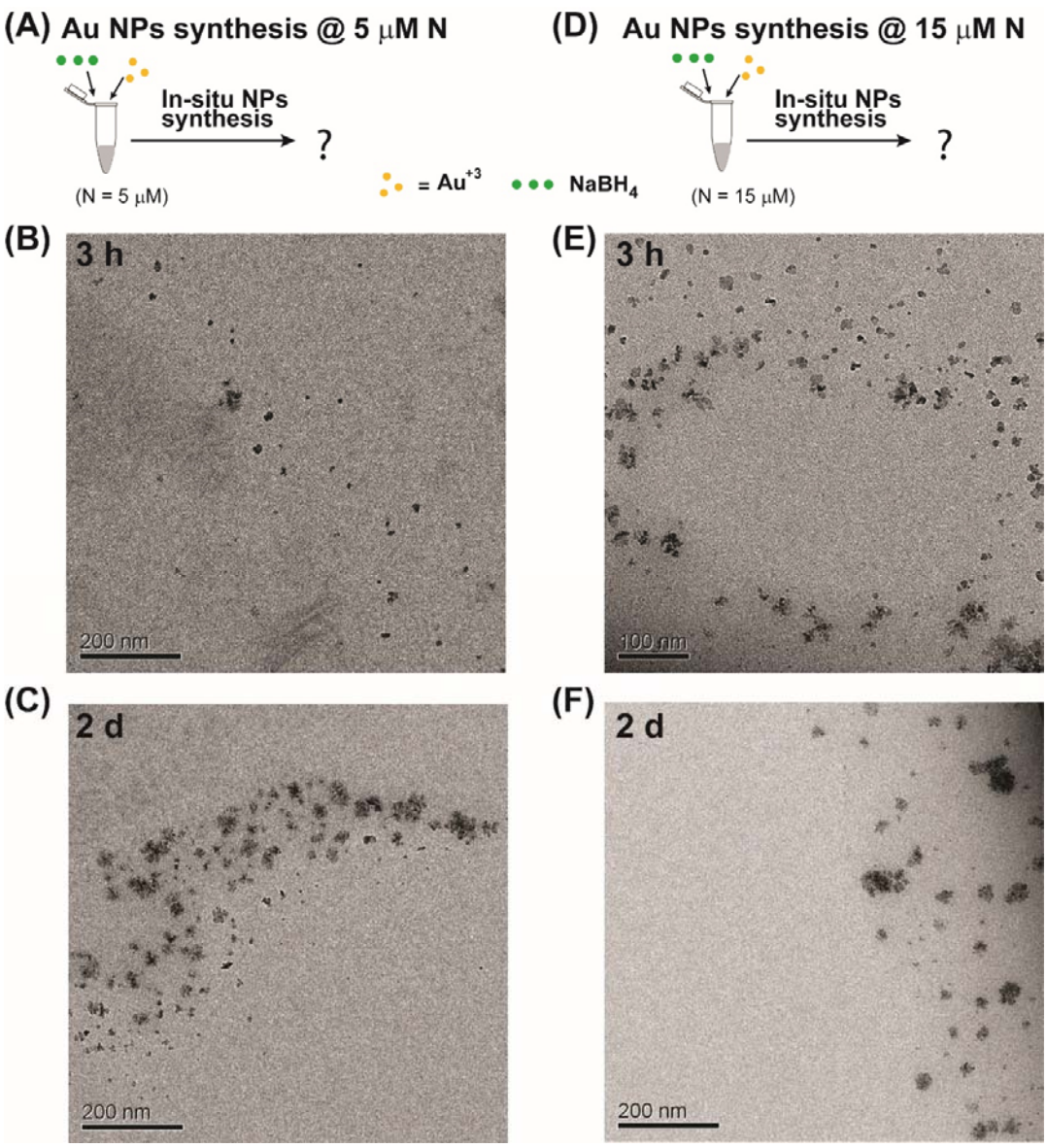

Figure s7. (A) Au NPs synthesis in 5 μM mixtures of **N**, corresponding to its abundance in the Hss. **(B)** & **(C)** TEM images denoting the NP morphologies after 3h and 2d of incubation. **(D)** Au NPs synthesis in 15 μM mixtures of **N** corresponding to its abundance in Lss. **(E)** & **(F)** TEM images denoting the NP morphologies after 3h and 2d of incubation. In all experiments, the concentration of Au salt and $NaBH_4$ were maintained as 15 μM and 500 μM, respectively. Experiments were carried out at room temperature 22 °C.

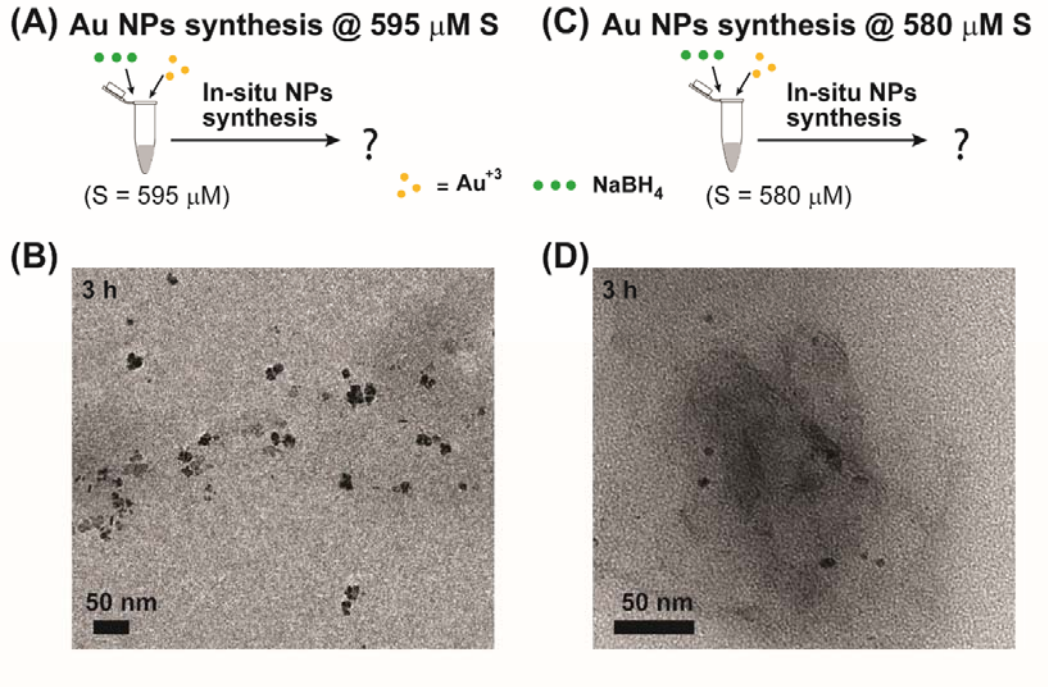

Figure s8. (A) Au NPs synthesis in 595 μM mixtures of **S**, corresponding to its abundance in the Hss. **(B)** TEM image denoting the NP morphologies after 3h of incubation. **(C)** Au NPs synthesis in 580 μM mixtures of **S** corresponding to its abundance in Lss. **(D)** TEM images denoting the NP morphologies after 3h of incubation. In all experiments, the concentration of Au salt and $NaBH_4$ were maintained as 15 μM and 500 μM, respectively. Experiments were carried out room temperature 22 °C.

5.6 Analyzing the preferences of different network components towards Au NPs surface functionalization

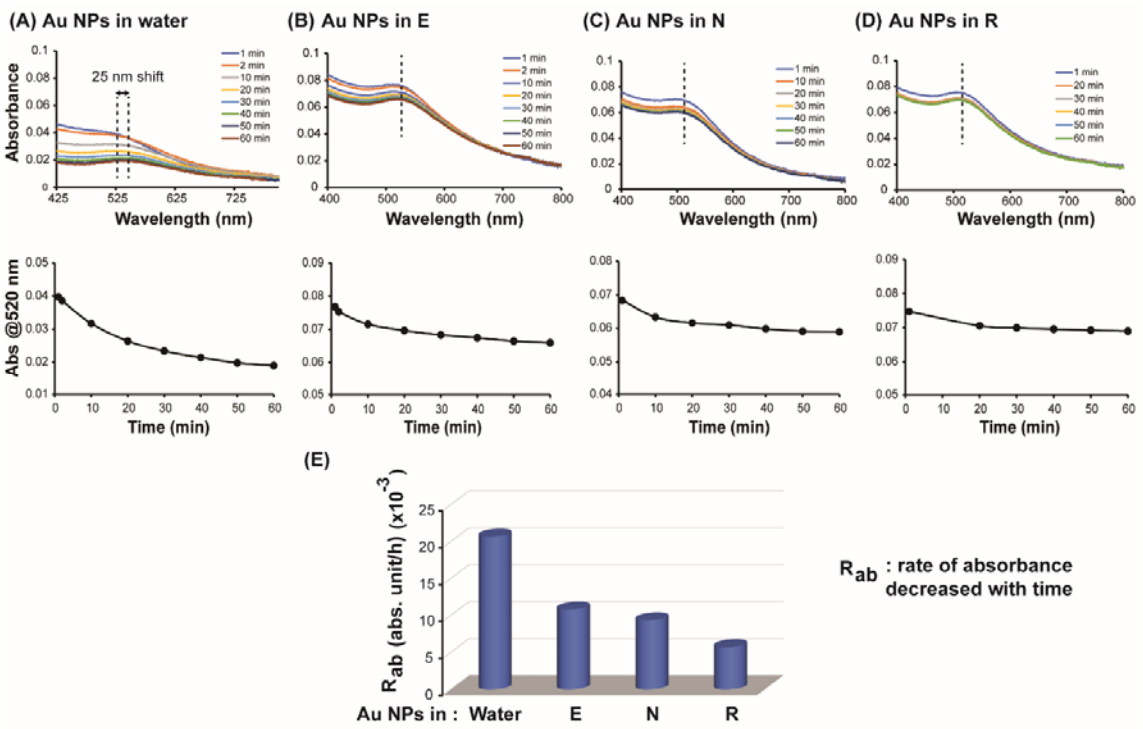

Figure s9: Real time absorbance (upper panels) and aggregation kinetics (deduced from the absorbance decrease; bottom panels) of 30 µM Au NPs investigated in water **(A)**, or in 100 µM mixtures of **E (B)**, **N (C)**, and **R (D)**. **(E)** The respective rate of aggregation in pure water or in mixtures of the individual components **E**, **N** and **R.** The Au NPs are prepared in water by reducing $AuCl_3$ with $NaBH_4$

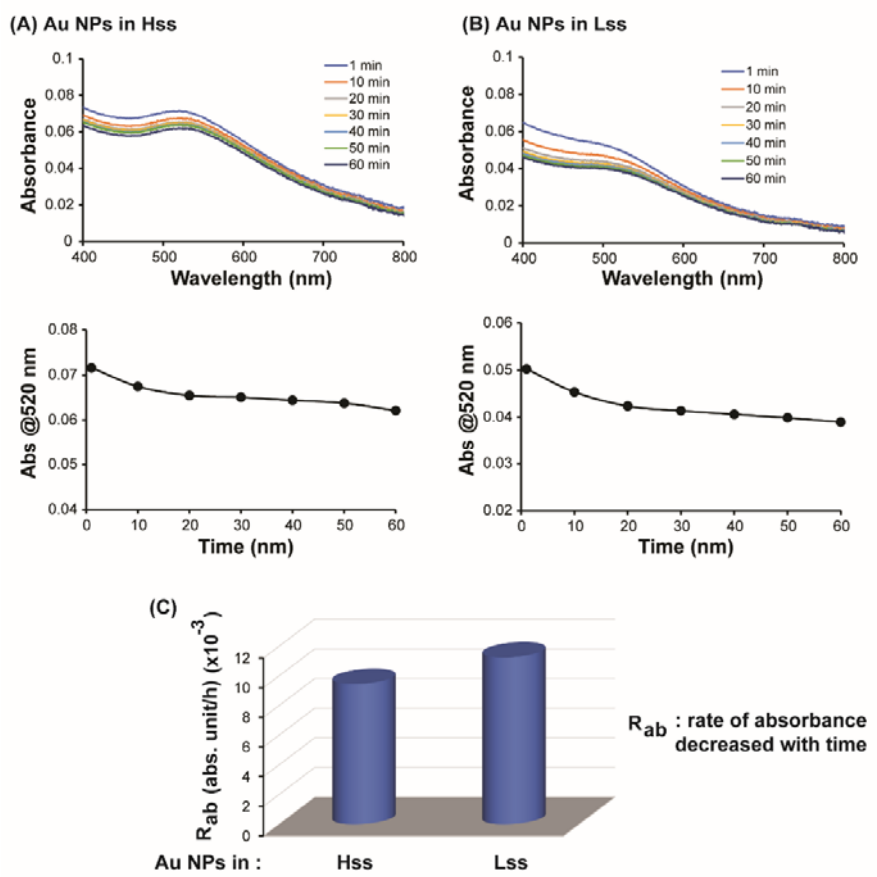

Figure s10: The real time absorbance (upper panel) and aggregation kinetics (deduced from the absorbance decrease; bottom panel) of 30 µM of Au NPs investigated in **(A)** Hss and **(B)** Lss mixtures. **(C)** The respective rate of aggregation in the Hss and Lss mixtures**.** The Au NPs are prepared in water by reducing $AuCl_3$ with $NaBH_4$.

5.7 Characterizing the nanoparticle red and blue seeds

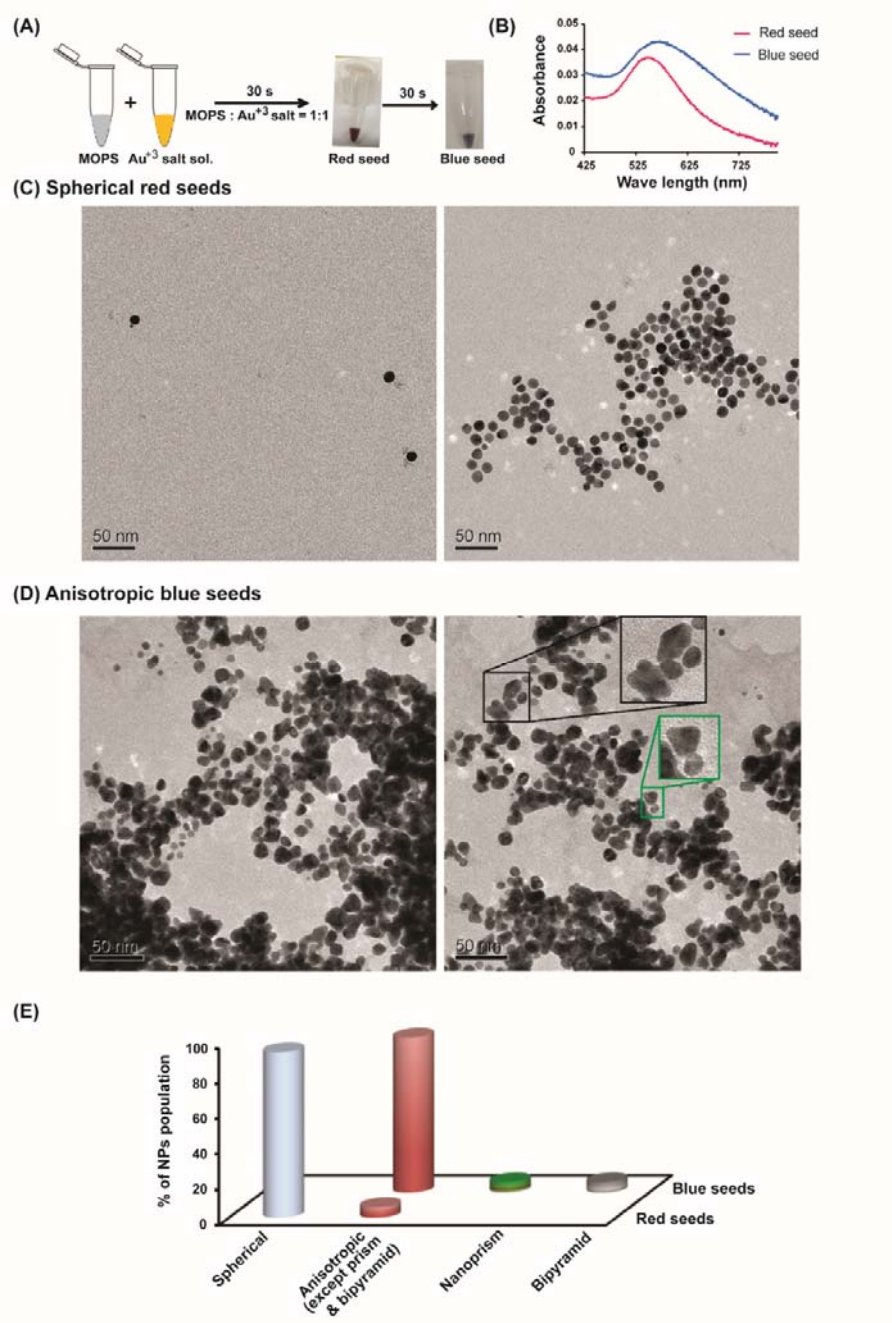

Figure s11. **(A)** Preparation of the Au NP red and blue seeds by mixing 1:1 (v/v) MOPS buffer (500 mM, pH =7) and stock solutions of Au salt (4500 μM). **(B)** UV-Vis spectra highlighting the characteristic peak of the red seeds absorption at 532 nm, and the surface plasmon resonance peak of the blue seeds at 575 nm. For these UV-Vis experiments, the two seed type solutions were diluted in distilled water to a final concentration of 30 μM. **(C)** & **(D)** TEM images showing the spherical red seeds and anisotropic blue seeds, respectively. **(E)** Relative population of the spherical and anisotropic NPs found in red and blue seeds mixtures, respectively. More than 250 NP objects were manually screened for this calculation.

5.8 Controlling the self-assembly of Au nanoparticles

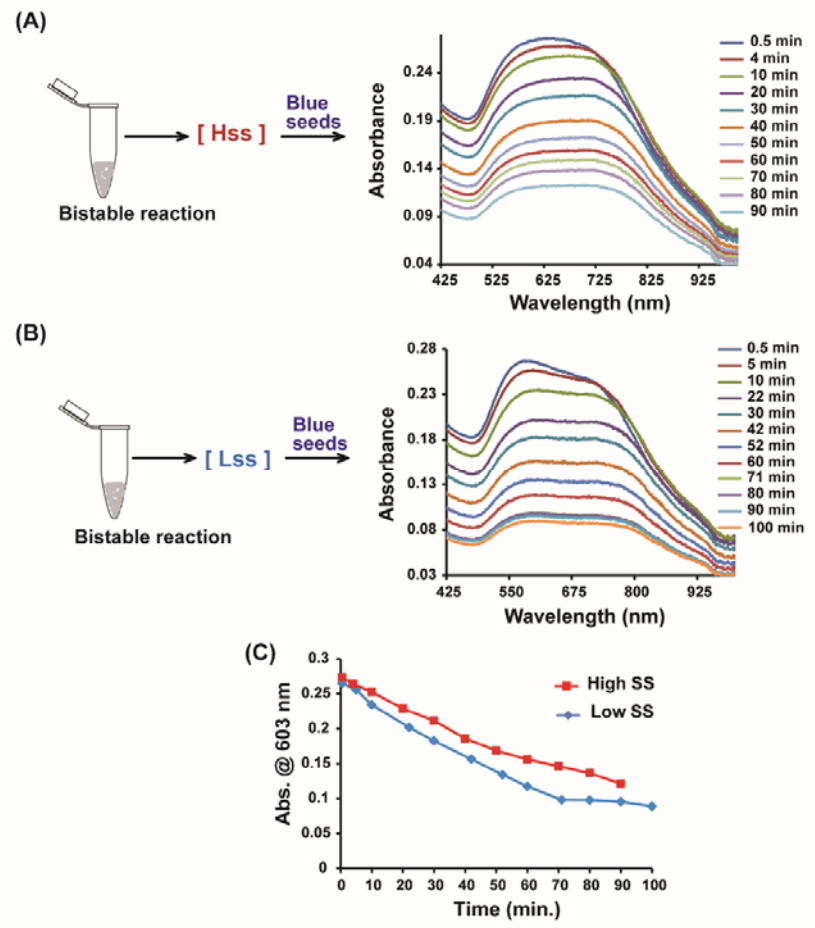

Figure s12. (A) & **(B)** UV-Vis spectra highlighting the real-time aggregation kinetics of the bluish anisotropic Au NP seeds in the Hss and Lss, respectively. **(C)** Surface plasmon resonance absorption as a function of time for blue Au NP seeds incubated in the Hss and Lss. The NRG processes were carried out separately to follow the self-assembly behavior of Au NPs in these respective SSs with 100 μM of Au blue seeds at pH=7 and 22 °C.

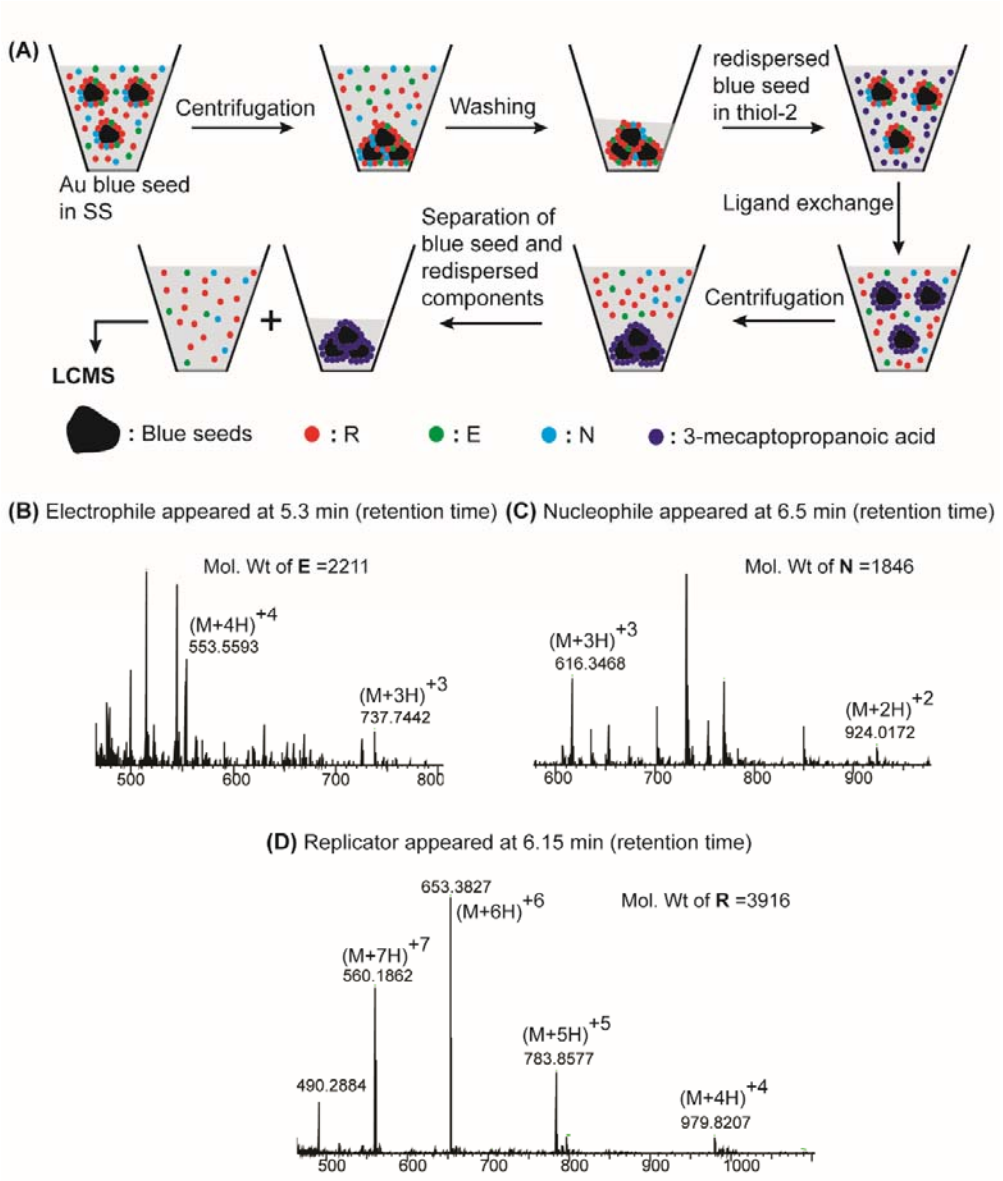

Figure s13. (A) general layout of ligand the exchange experiments applied to identify the Au NPs bound network components. LCMS (liquid chromatography mass spectrometry) analysis featuring relatively small peaks of both the **E (B)** and **N (C)** and larger peaks corresponding to replicator **R (D)**, suggesting that **R** has functionalized the Au NPs to a higher extent than the other network components.

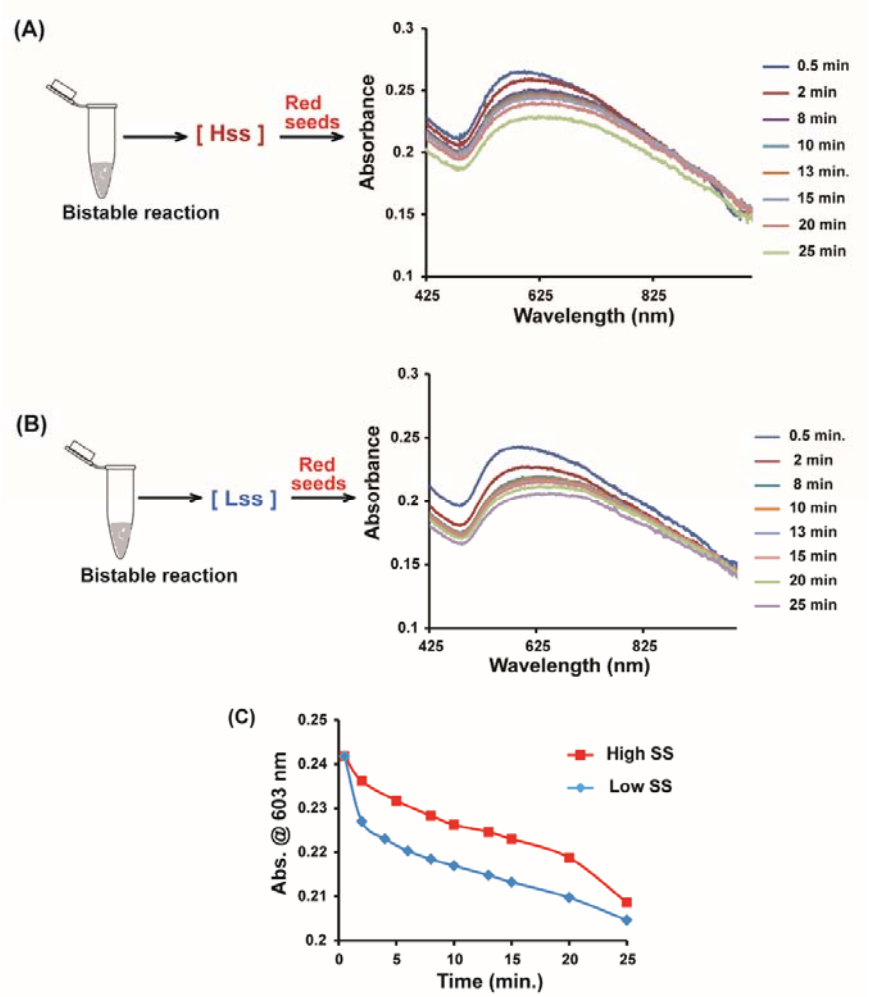

Figure s14. (A) & **(B)** UV-Vis spectra highlighting the real-time aggregation kinetics of the spherical red Au NP seeds in the Hss and Lss, respectively. **(C)** The surface plasmon resonance absorption as a function of time for spherical red Au NP seeds incubated in the Hss and Lss. The NRG processes were carried out separately to follow the self-assembly behavior of Au NPs in these respective SSs with 100 μM of Au red seeds at pH=7 and 22 °C.

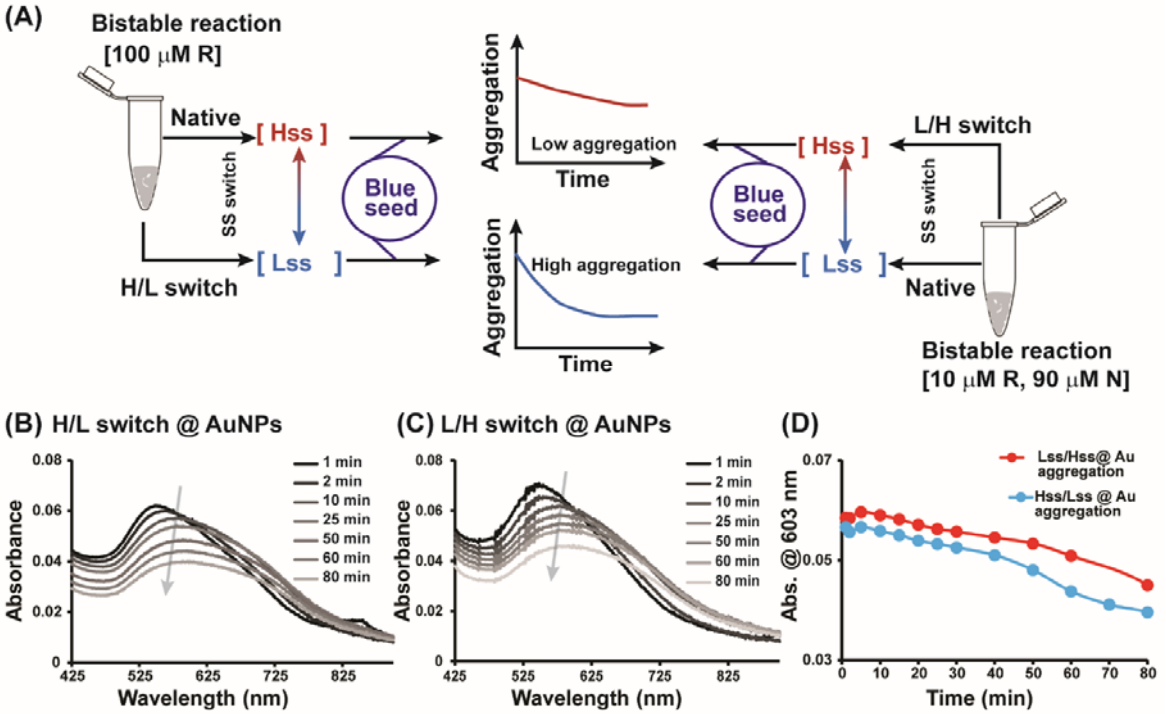

Figure s15. (A) Scheme presenting that the native Hss and Lss induce slow and faster aggregation of Au NPs blue seeds, respectively. As expected, the switched Hss-to-Lss mixture shows faster aggregation kinetics versus the Lss-to-Hss switched mixture. **(B, C)** UV-Vis spectra that allowed to follow the real time aggregation of bluish Au NP seeds within the Hss-to-Lss switch and Lss-to-Hss switch mixtures, respectively. **(D)** Au NP plasmon resonance absorption (603 nm) as a function of time, extracted from the data shown in **(B)** and **(C).** The NRG processes were carried out in the respective SS mixtures with 30 μM of Au blue seeds (anisotropic NP seeds) at pH=7 and 22 °C

5.9 Long term stability of the network components in presence of Au NPs

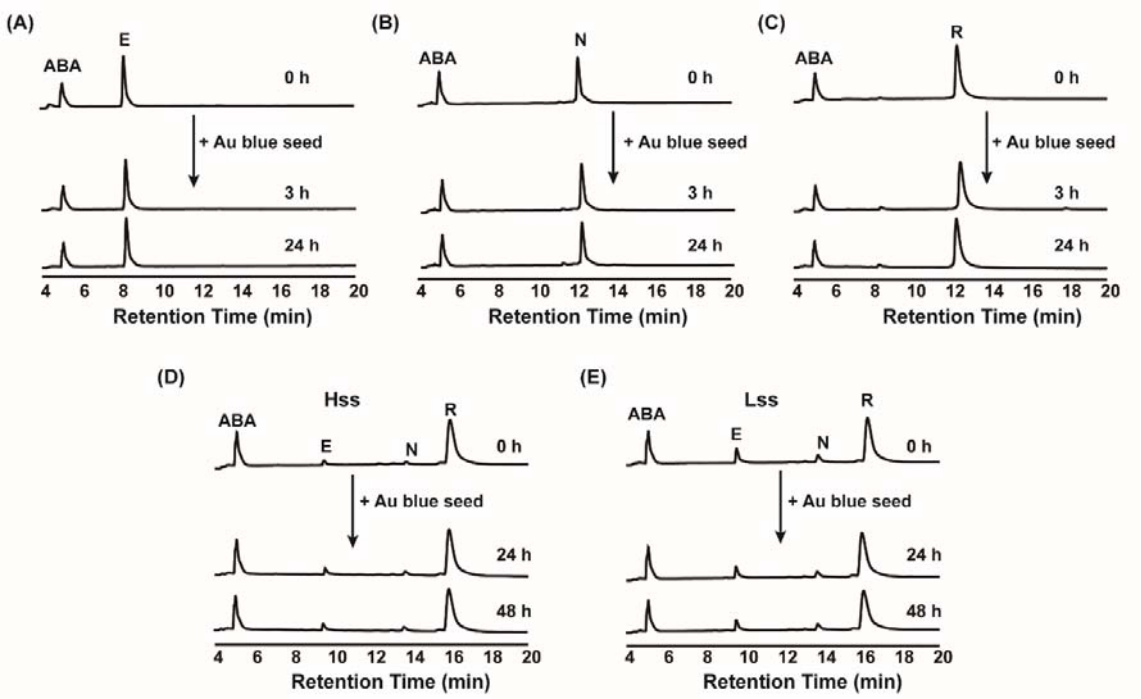

Figure s16. (A-C) HPLC chromatograms show that the networks components (**E**, **N** and **R**) were not affected by subjection of Au NPs during the experiments. **(D)** and **(E)** confirm that the respective Hss and Lss components distribution were not changed during these experiments**.** We note that (when neede) different HPLC gradient programs were used for studying the different mixtures.

5.10 Controlling the shape of Au nanoparticles

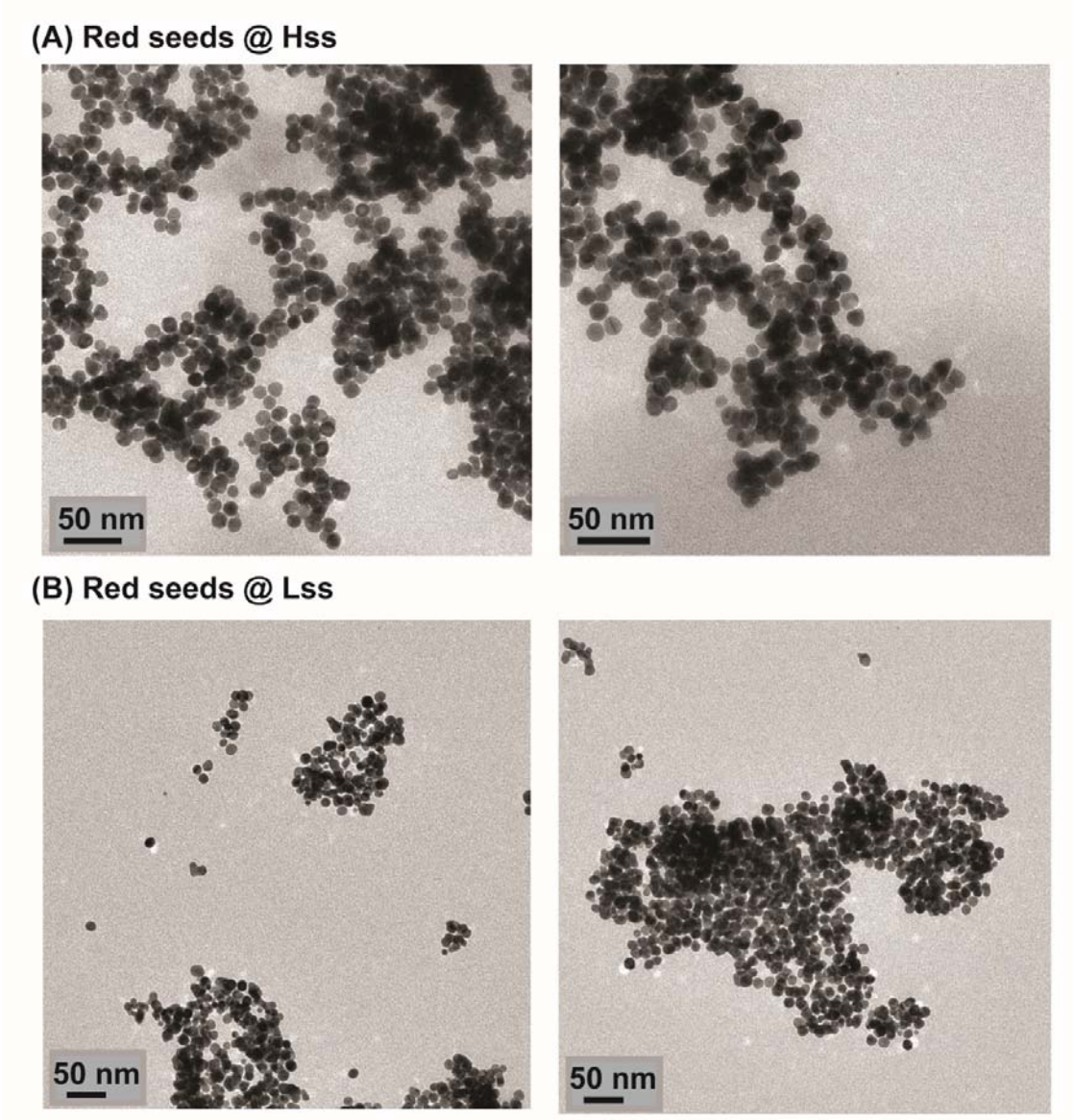

Figure s17. (A) and **(B)** TEM images of Au NPs obtained after 2 days of incubation of the red seeds in the Hss and Lss mixtures, respectively. The NRG processes were carried out in the respective SS mixtures with 100 μM of Au red seeds at pH=7 and 22 °C.

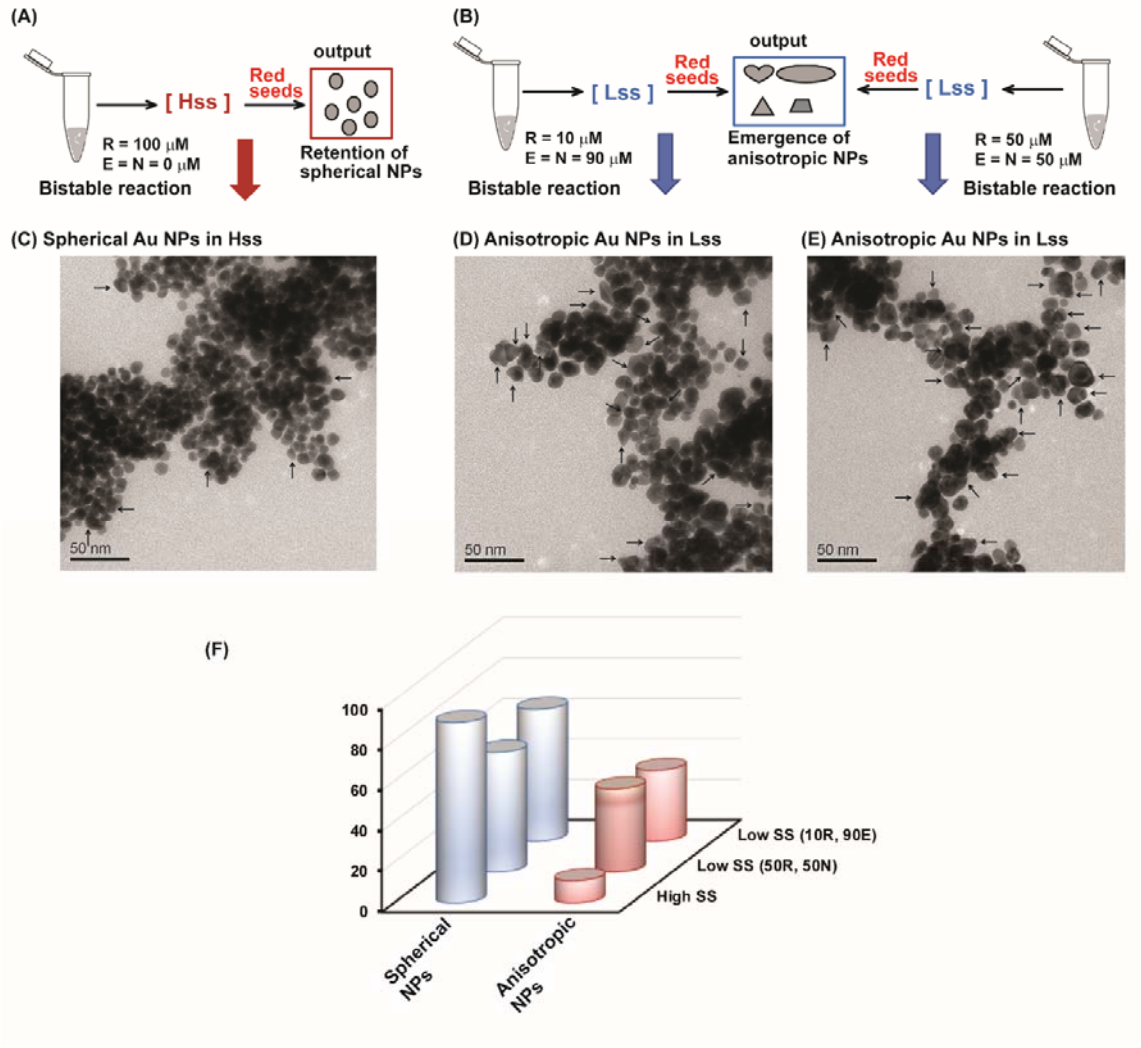

Figure s18. (A) Replication reaction initiated with 100 μM **R** yielding the Hss, which is used to investigate the shape controlling behavior of the bistable network reaction. **(B)** Replication reaction initiated with either 10 μM of **R** and 90 μM (each) of **E** and **N** or 50 μM of **R** and 50 μM (each) of **E** and **N** gives the Lss, which is used to investigate the shape controlling behavior. In these experiments 30 μM of pre-synthesized Au NP red seeds were cultivated in the respective steady state mixtures for 2 days. **(C)** TEM images of Au NP red seeds cultivated in the Hss, revealing that the spherical shape was retained. **(D)** & **(E)** TEM images of Au NP red seeds cultivated in the Lss, obtained from both the above input signals given in (B), showing the emergence of anisotropic Au NPs. Selected anisotropic NPs are marked by the black arrows. **(E)** Relative population of the spherical and anisotropic NPs in the Hss and Lss mixtures. For NP shape population calculation, more than 100 NPs are manually screened.

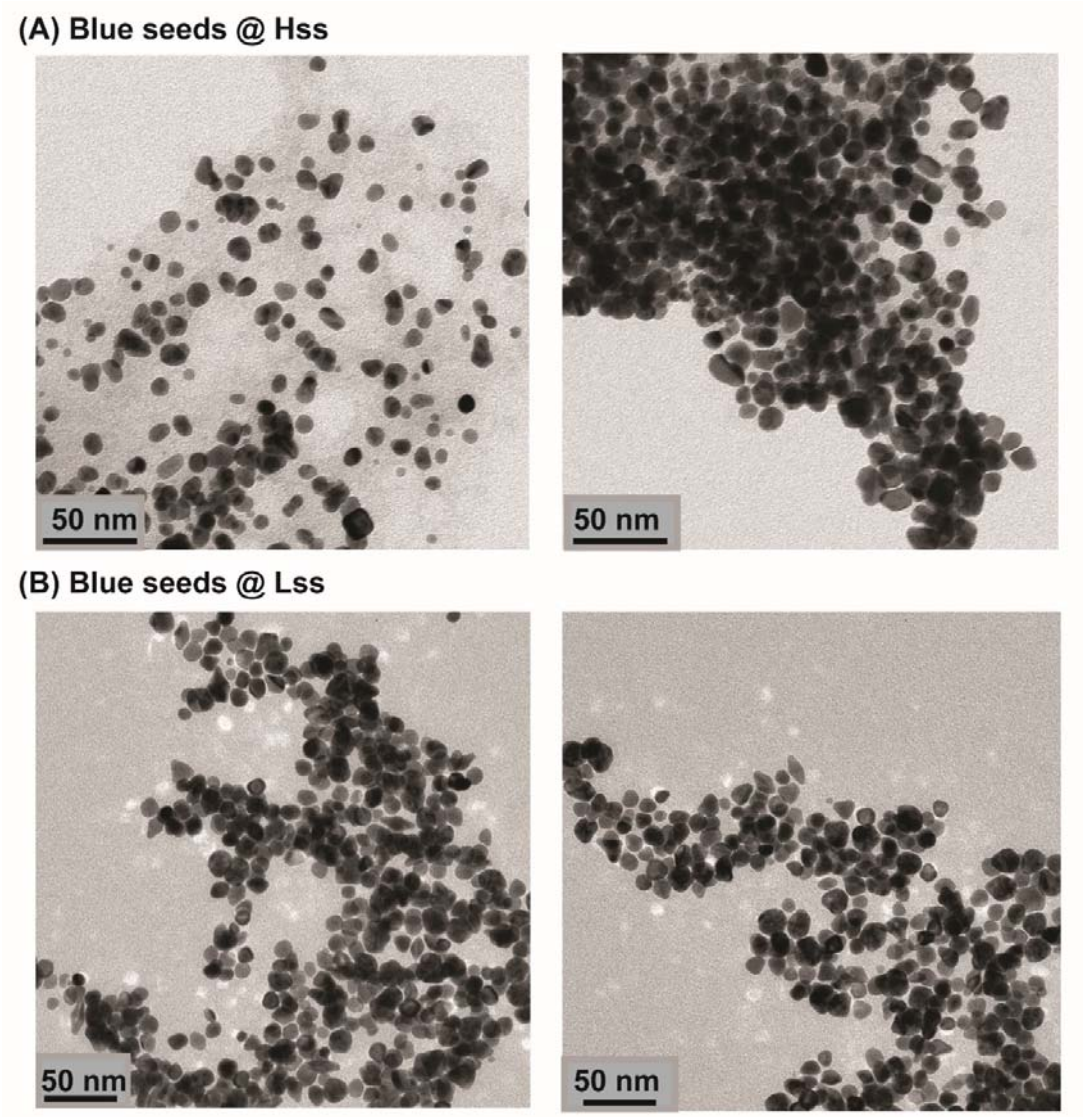

Figure s19. (A) and **(B)** TEM images of Au NPs obtained after 2 days of incubation of the blue seeds in the Hss and Lss mixtures, respectively. The NRG processes were carried out in the respective SS mixtures with 100 μM of Au blue seeds at pH=7 and 22 °C.

6. References

[1] Z. Dadon, M. Samiappan, A. Shahar, R. Zarivach, G. Ashkenasy, *Angew. Chem. Int. Ed.* **2013**, *52,* 9944-9947.
[2] R. Mukherjee, R. Cohen-Luria, N. Wagner, G. Ashkenasy, *Angew. Chem. Int. Ed.* **2015**, *54*, 12452-12456.
[3] I. Maity, N. Wagner, R. Mukherjee, D. Dev, E. Peacock-Lopez, R. Cohen-Luria, G. Ashkenasy, *Nat. Commun.* **2019**, *10*, 4636.
[4] A. Chotera, H. Sadihov, R. Cohen-Luria, P. A. Monnard, G. Ashkenasy, *Chem. Eur. J.* **2018**, *24*,10128 –10135.